Mechanism of the migration of the substituent in 1,2,3,7a-tetrahydroimidazo[1,2-*b*]isoxazole derivatives

N. V. Chukanov,[a,b] S. A. Popov,[b] T. N. Drebushchak,[a,c] and V. A. Reznikov[a,b]*

[a]*Novosibirsk State University,*
2 ul. Pirogova, 630090 Novosibirsk, Russian Federation.
Fax: +7 (383) 330 2237. E-mail: decan@fen.nsu.ru
[b]*N. N. Vorozhtsov Novosibirsk Institute of Organic Chemistry, Siberian Branch of the Russian Academy of Sciences,*
9 prosp. Akad. Lavrent´eva, 630090 Novosibirsk, Russian Federation.
Fax: +7 (383) 330 9752. E-mail: nikita@nioch.nsc.ru
[c]*Institute of Solid State Chemistry and Mechanochemistry, Siberian Branch of the Russian Academy of Sciences,*
18 ul. Kutateladze, 630128 Novosibirsk, Russian Federation.
Fax: +7 (383) 332 1550. E-mail: tanya@xray.nsu.ru

The thermolysis of 1,2,3,7a-tetrahydroimidazo[1,2-*b*]isoxazole derivatives results in intramolecular rearrangements by two main pathways. One rearrangement affords azomethine ylide derivatives. Another rearrangement leads to the migration of the substituent from position 7a to the nitrogen atom. The rate constants of these reactions were determined. Quantum chemical calculations by the DFT method were carried out. Based on the data for the migration of the substituent, the concerted mechanism was proposed.

Key words: 2,3-dihydroisoxazole, 1,2,3,7a-tetrahydroimidazo[1,2-*b*]isoxazole, sigmatropic rearrangement, azomethine ylide, rate constants, quantum chemical calculations, DFT method, X-ray diffraction study.

Previously, we have shown[1] that the thermolysis of 1,2,3,7a-tetrahydroimidazo[1,2-*b*]isoxazole derivatives **1**, which were synthesized by the 1,3-dipolar cycloaddition of nitrones of the 2-imidazoline series with alkynes (Scheme 1), results in their rearrangement into ylides **3** (path *a*) and/or the migration of the substituent from position 7a of compound **1** to the nitrogen atom N(4) to form imidazolidines **4** (path *b*). Previously, the formation of azomethine ylides has been observed for a wide range of 2,3-dihydroisoxazole derivatives,[2—7] or these compounds were assumed to be intermediates in the formation of oxazole and pyrrole derivatives and in other rearrangements of 2,3-dihydroisoxazoles. The hydrogen migration is the well-known transformation of bicyclic 2,3-dihydroisoxazole derivatives.[8—11] However, the migration of the substituent containing the sp^3-hybridized[12,13] or sp^2-hybridized[14,15] carbon atom was observed only for a few substantially structurally different compounds. Hence, it was impossible to draw a conclusion about the mechanism of this reaction. We revealed for the first time the general character of this process in the study of 2,2,3,3-tetramethyl-7a-R-1,2,3,7a-tetrahydroimidazo[1,2-*b*]isoxazole derivatives **1** and synthesized a series of migration products of the substituent R (the structure of one of these products, **4k**, was confirmed by X-ray diffraction, Fig. 1).[1] The aim of the present study was to reveal the kinetic features of the reaction and elucidate the mechanism of the rearrangement (see Scheme 1) following the path *b* with the use of DFT calculations.

The rectification of the kinetic curves in the ln*k*—*t* coordinates (*k* is the reaction rate constant, and *t* is the reaction time) showed that the reactions *a* and *b* (see Scheme 1) are first order with respect to the reagent. The concentrations of the components were determined by ^{1}H

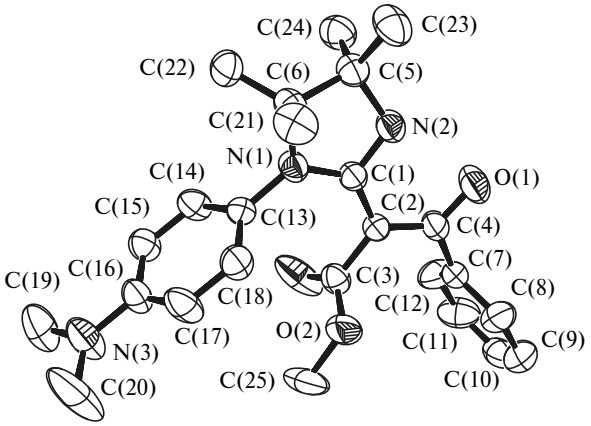

Fig. 1. Molecular structure of compound **4k** (thermal ellipsoids are drawn at the 30% probability level). The hydrogen atoms are not shown.

Published in Russian in *Izvestiya Akademii Nauk. Seriya Khimicheskaya,* No. 9, pp. 1769—1777, September, 2010.
1066-5285/10/5909-1817

Scheme 1

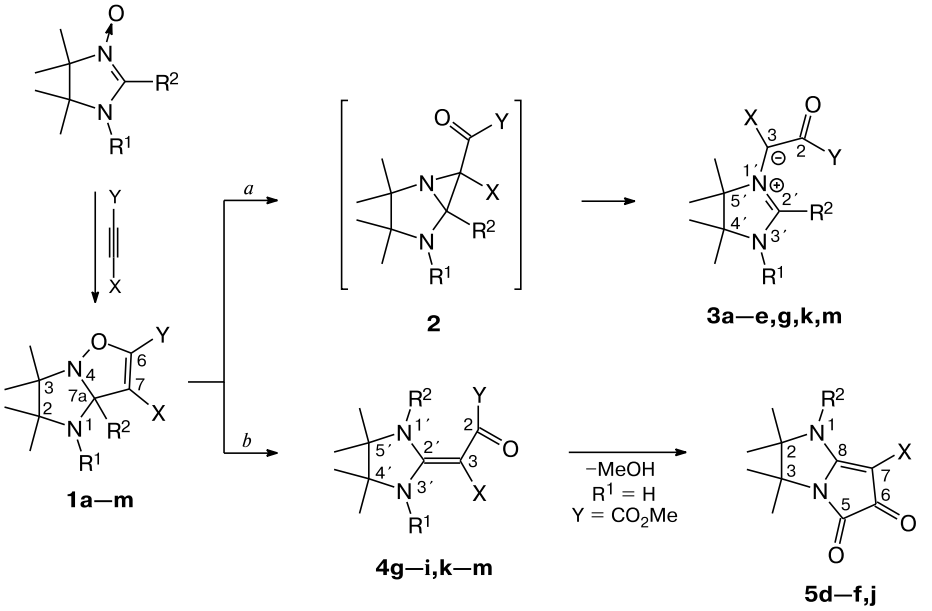

1	R^1	R^2	X	Y	**1**	R^1	R^2	X	Y
a	H	Me	CO_2Me	CO_2Me	**h**	Me	Ph	CO_2Me	CO_2Me
b	H	Bu^t	CO_2Me	CO_2Me	**i**	Me	4-MeO-C_6H_4	CO_2Me	CO_2Me
c	H	4-NO_2-C_6H_4	CO_2Me	CO_2Me	**j**	H	—CH=CH—Ph	CO_2Me	CO_2Me
d	H	Ph	CO_2Me	CO_2Me	**k**	H	4-Me_2N-C_6H_4	CO_2Me	Ph
e	H	4-MeO-C_6H_4	CO_2Me	CO_2Me	**l**	H	4-Me_2N-C_6H_4	COMe	Ph
f	H	4-Me_2N-C_6H_4	CO_2Me	CO_2Me	**m**	H	4-Me_2N-C_6H_4	CN	Ph
g	Me	4-NO_2-C_6H_4	CO_2Me	CO_2Me					

NMR spectroscopy of the reaction mixtures based on the integrated intensities of the signals of the reaction products and the reagent. The rate constants k_a and k_b for the parallel reactions were calculated by the equations (1) and (2), respectively.

$$\mathbf{A} \xrightarrow{k_a} \mathbf{B}$$
$$k_a = kB/(B + C), \quad (1)$$

where $k = k_a + k_b = (1/t)\ln[A/(A + B + C)]$.

$$\mathbf{A} \xrightarrow{k_b} \mathbf{C}$$
$$k_b = kC/(B + C) \quad (2)$$

A, B, and C are the integrated intensities of compounds **1**, **3**, and **4** (**5**), respectively, and t is the reaction time.

The formation of azomethine ylides **3** is associated with the rearrangement presented in Scheme 1 (path *a*), which apparently occurs through the initial formation of aziridine **2** followed by its cleavage. According to the published data, the concerted[16] or non-concerted biradical[17] pathways of the formation of the aziridine ring are the most probable mechanisms. The absence of signals of acylaziridine **2** in the ^{1}H NMR spectra of the reaction mixtures indicates that the formation of this compound is the rate-limiting step (assuming that the reaction actually occurs through this compound). It was shown that the polarity of the solvent (Table 1) and the nature of the substituent R^2 (Table 2, see Scheme 1) have an insignificant effect on the rate of the reaction *a*.

The above-considered data do not contradict both the concerted and biradical pathways of the formation of acylaziridine. However, these data are inconsistent with the reaction proceeding *via* the zwitterion; otherwise, the polarity of the solvent would substantially influence the reaction rate.

Table 1. Dependence of the rate constant k_a of the reaction *a* for compound **1d** on the nature of the solvent at 105 °C

Solvent	ε*	$k_a \cdot 10^6/s^{-1}$
CCl_4	2.28	3.0±0.4
Toluene	2.38	9.3±0.9
Acetone	20.7	5.6±0.5
DMSO	49	7.6±0.6

* ε is the dielectric permeability.

Table 2. Dependence of the rate constant k_a of the reaction *a* on the nature of the substituent R^2 for compounds **1a—e** in toluene

R^2	$k_a \cdot 10^5/s^{-1}$	
	131 °C	105 °C
Me	—	0.55±0.02
Bu^t	—	1.5±0.05
p-NO_2—C_6H_4	7.4±0.1	—
Ph	11.8±0.2	0.93±0.09
p-MeO—C_6H_4	14.0±0.2	—

It should be noted that the thermolysis of compound **1l** affords the migration product of the substituent **4l** along with ylide **3l**; however, the latter compound undergoes the ketone cleavage to form ylide **3l′** in the course of the isolation (Scheme 2). The structure of **3l′** was confirmed by ^1H and ^{13}C NMR spectroscopy, in particular, by the absence of the signals of the acetyl group and the presence of the signal for H(2) at δ_H 4.91, as well as by the high-resolution mass spectrum.

Scheme 2

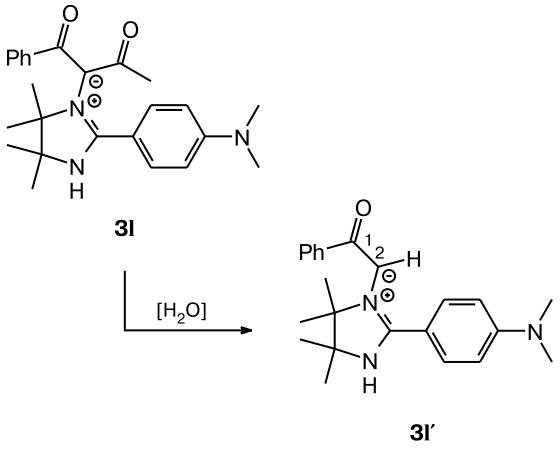

Table 3 presents the kinetic data on the influence of the polarity of the solvent on the rate constant of the migration of the substituent in compounds **1d**, **1e**, and **1f** (reaction *b*, see Scheme 1).

The rate of this rearrangement substantially increases with an increase in the polarity of the solvent, which is indicative of the high polarity of the transition state of the reaction.

The data on the influence of the substituents R^1 and R^2 on the reaction rate at different temperatures are presented in Table 4. The Gibbs energies ($\Delta G^{\#}_{298}$), the enthalpies ($\Delta H^{\#}_{298}$), and the entropies ($\Delta S^{\#}_{298}$) of activation were calculated by the Eyring equation ($\ln k = \ln(\kappa T/h) - (\Delta G^{\#}_{298}/RT)$).

It was found that an increase in the π-donor ability of the substituent R^2 leads to an increase in the rate of its migration. The influence of the substituent Z in the *para* position of the phenyl ring (Scheme 3) correlates with the Hammett constants σ^+,[18] which provides an estimate of the sensitivity of the reaction (ρ) in two reaction series, which are −3.2 (R^1 = H, X = Y = CO_2Me) and −2.3 (R^1 = Me, X = Y = CO_2Me), respectively (Fig. 2).

It is worthy of note that the activation barrier for the migration of the styryl group (R^2 = —CH=CH—Ph, **1j**) in position 7a is 3 kcal mol^{-1} lower than that for the phenyl group (R^2 = Ph, **1d**) (see Table 4).

The ease of the migration of the substituent R^2 substantially depends also on the nature of the substituent R^1. Thus, the introduction of the methyl group at the nitrogen atom N(1) (**1h**, **1i**) leads to a decrease in the activation barrier by approximately 2 kcal mol^{-1} compared to the N-unsubstituted compounds (**1d**, **1e**).

There are the following three most probable mechanisms of the rearrangement: the non-concerted pathway either through biradical intermediate **6** (see Scheme 3, path *a*) or through zwitterionic intermediate **7** (path *b*) and the concerted pathway through transition state **8** (Scheme 4).

As a rule, the polarity of the solvent has no substantial effect on radical reactions, whereas the rate of these reactions substantially increases when nonpolar CCl_4 is replaced by DMSO (see Table 3). In addition, the substituents Z of any nature in the *para* position of the phenyl moiety R^2 should facilitate the formation of biradical in-

Table 3. Dependence of the rate constant k_b of the reaction *b* for compounds **1d**, **1e**, and **1f** on the nature of the solvent

Solvent	ε	$k_b \cdot 10^4/s^{-1}$			
		1d		**1e** (131 °C)	**1f** (20 °C)
		105 °C	131 °C		
CCl_4	2.28	(0.5±0.1)·10^{-2}	—	—	(7.6±0.5)·10^{-3}
Toluene	2.38	(1.6±0.1)·10^{-2}	(2.0±0.1)·10^{-1}	2.3±0.2	(3.2±0.2)·10^{-2}
Acetone	20.7	(2.2±0.3)·10^{-2}	—	—	(1.3±0.1)·10^{-1}
DMSO	49	(14.0±0.3)·10^{-2}	17±2	21±2	1.0±0.1

Scheme 3

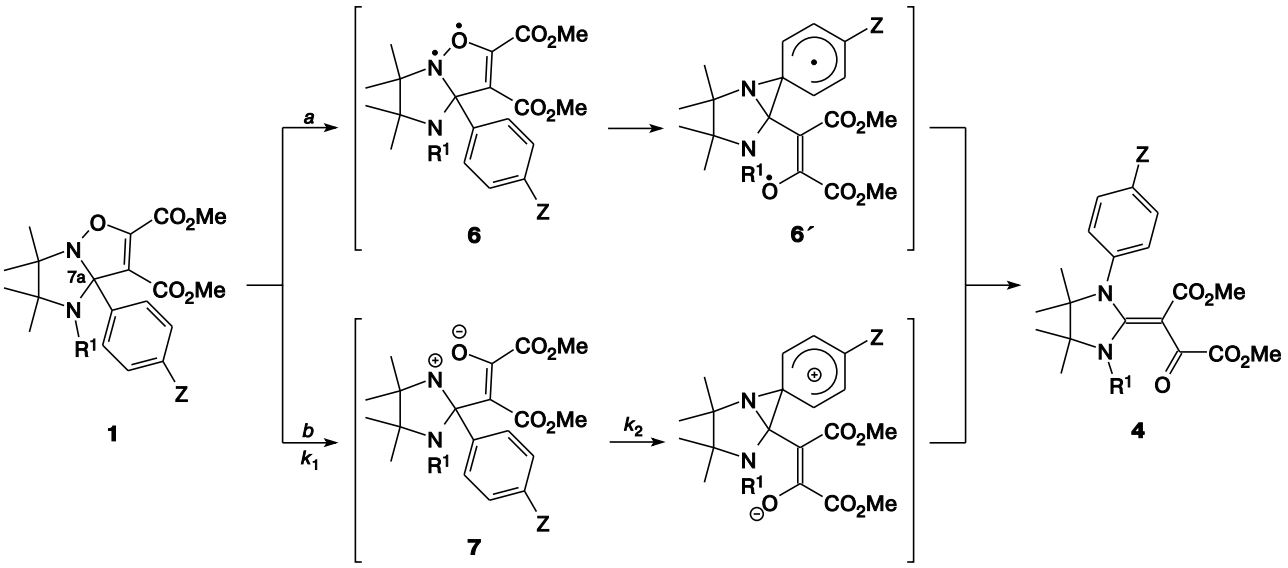

Table 4. Dependence of the rate constant k_b of the reaction *b* on the nature of the substituents R^1 and R^2 at different temperatures for compounds **1d—j** in toluene

R^2	T/K	k_b/s^{-1}	$\Delta G^{\#}_{298}$ /kcal mol^{-1}	k_b (298)[a] /s^{-1}
1d	378	$(1.6\pm0.1)\cdot10^{-6}$	32.1[b]	$2.5\cdot10^{-11}$
	394	$(7.4\pm0.2)\cdot10^{-6}$		
	404	$(2.0\pm0.1)\cdot10^{-5}$		
	413	$(4.6\pm0.2)\cdot10^{-5}$		
	423	$(9.7\pm0.7)\cdot10^{-5}$		
1e	358	$(3.6\pm0.1)\cdot10^{-6}$	29.4	$2.1\cdot10^{-9}$
	378	$(2.0\pm0.2)\cdot10^{-5}$		
	404	$(2.3\pm0.2)\cdot10^{-4}$		
1f[c]	293	$(3.2\pm0.2)\cdot10^{-6}$	24.6	$5.6\cdot10^{-6}$
	333	$(1.9\pm0.1)\cdot10^{-4}$		
	353	$(1.1\pm0.1)\cdot10^{-3}$		
1j	358	$(9.5\pm0.5)\cdot10^{-6}$	29.0	$4.2\cdot10^{-9}$
	378	$(6.7\pm0.7)\cdot10^{-5}$		
	404	$(7.4\pm0.2)\cdot10^{-4}$		
1g	378	$(1.4\pm0.1)\cdot10^{-6}$	32.1	$2.5\cdot10^{-11}$
	404	$(2.0\pm0.2)\cdot10^{-5}$		
	423	$(1.1\pm0.1)\cdot10^{-4}$		
1h	358	$(2.3\pm0.1)\cdot10^{-6}$	29.9	$9.4\cdot10^{-10}$
	378	$(3.9\pm0.2)\cdot10^{-5}$		
	404	$(4.9\pm0.5)\cdot10^{-4}$		
1i	333	$(4.3\pm0.2)\cdot10^{-6}$	27.6	$4.2\cdot10^{-8}$
	353	$(3.7\pm0.2)\cdot10^{-5}$		
	378	$(4.8\pm0.2)\cdot10^{-4}$		

[a] The rate constants are reduced to the temperature of 298 K.
[b] $\Delta H^{\#}_{298}$ = 30.8 kcal mol^{-1}, $\Delta S^{\#}_{298}$ = −4.4 cal mol^{-1} K.
[c] In deuteriotoluene.

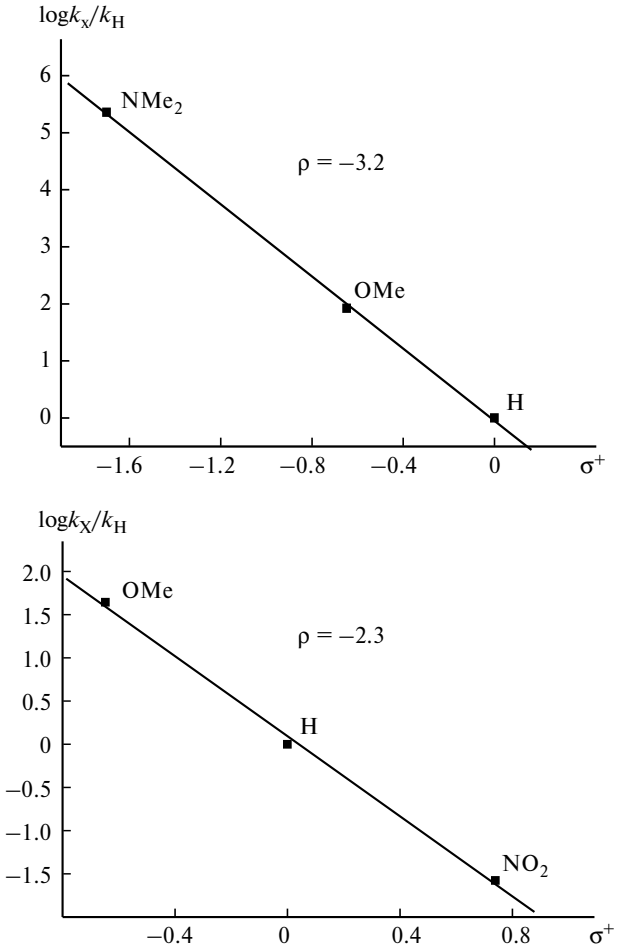

Fig. 2. Sensitivity of the reaction (ρ) to the substituent Z for compounds **1d—f** and **1g—i** at 25 °C.

Scheme 4

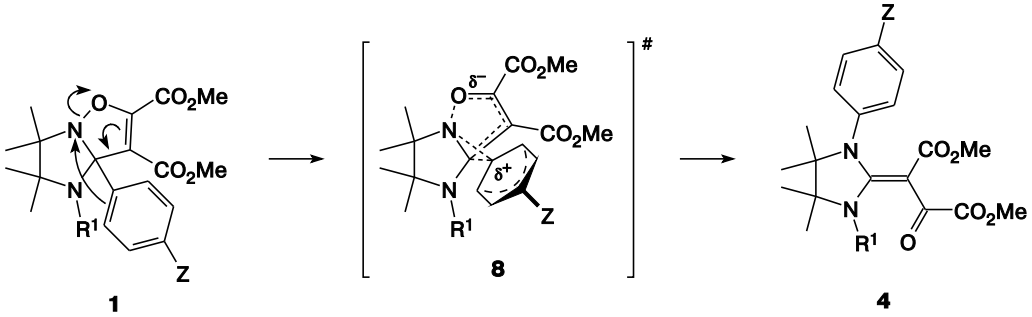

termediate **6´**, which is inconsistent with the experimental data. The N—O bond cleavage is not the rate-limiting step of the reaction; otherwise, the nature of the substituent Z would have no effect on the reaction rate. Hence, the path *a* (see Scheme 3) is unlikely to occur.

Since the signals of intermediate **7** are absent in the ^{1}H NMR spectra of the reaction mixtures, it is necessary to analyze the following two alternative situations for the evaluation of the possibility of the zwitterion mechanism (see Scheme 3, path *b*): (1) the N—O bond cleavage giving intermediate **7** is the rate-limiting step (k_1) and (2) the migration of the substituent is the rate-limiting step (k_2). In the former case ($k_1 < k_2$), the π-donor effect of the substituent R^2 on the reaction rate would be insignificant, which is inconsistent with the experimental data (see Table 4). The second step involves the aromatic electrophilic substitution (electrophilic amination). The relatively low magnitudes of ρ (from *ca.* −2 to −3) compared to the known sensitivities of the electrophilic substitution in the aromatic series (ρ from *ca.* −6 to −12)[18,19] indicate that the transition state is earlier than that observed in usual electrophilic substitution reactions, and the degree of the positive charge transfer to the "σ complex" is lower. These values are also smaller than the sensitivity of the electrophilic amination by the reagents R_2NOX; in the case of phenylhydroxylamine, ρ = −5.2.[20] It should be noted that the formation of intermediate **7** can be accompanied by the generation of acylaziridines **2** in the competitive reaction, and in this case the reaction rate of the formation of the latter compounds would depend on the polarity of the solvent, which is inconsistent with the above-considered experimental data.

Therefore, the one-step reaction occurring through polar transition state **8** (see Scheme 4) seems to be the most probable process. In this transition state, the partial positive charge is delocalized on the N(4) and C(7a) atoms and the aromatic ring, and the negative charge is delocalized on the π system of the leaving group of activated complex **8**. This structure of the activated complex may be responsible for an increase in the reaction rate in polar solvents.

In terms of the polar transition state, the influence of the substituent R^2 can be explained as follows. Substituents with stronger donor properties in the aromatic ring (Z = OMe or NMe_2) stabilize the "σ complex" in the transition state, thus decreasing the activation energy and increasing the reaction rate. On the contrary, the strong acceptor (Z = NO_2) destabilizes this complex, thus decreasing the reaction rate.

The migration of the styryl group in the transition state should afford the analog of the benzyl cation **9** (Scheme 5), which is obviously energetically more favorable than the

Scheme 5

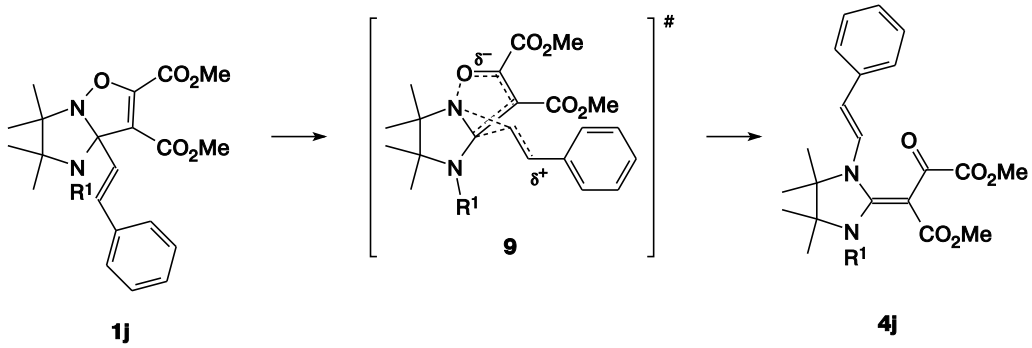

partial disturbance of the aromaticity in the route to "σ complex" **8** containing R^2 = Ph and is, apparently, responsible for an increase in the rate of migration in the case of compound **1j** compared to **1d**.

The substituents in positions 6 and 7 in molecule **1** should also influence the energetics of the transition state (and the reaction rate). Thus, the electron-withdrawing groups should stabilize the partial negative charge in the transition state and lead to an increase in the reaction rate. In the case of compound **1k** containing the substituent with weaker electron-withdrawing properties (phenyl group, Y = Ph) in position 6, the isomerization occurs approximately three orders of magnitude more slowly compared to compound **1f** (Y = CO_2Me). Substituents with stronger electron-withdrawing properties in position 7 in compounds **1l,m** (X = COMe or CN) increase the reaction rate of the rearrangement by a factor of 2—3 compared to compound **1k** (X = CO_2Me).

To explain the observed features of the migration of the substituent (see Scheme 1, reaction *b*) and to consider the reaction mechanism in detail, we performed quantum mechanical calculations for this process. The DFT calculations at the PBE level of theory with the 3z basis set gave the energy surface of the reaction (Fig. 3) in the coordinates of the breaking N—O bond (*d*) and the R^2—C—N bond angle (φ) (Fig. 4). The bond length *d*(N—O) and the bond angle φ(R^2—C—N) in the starting compound **1** were taken as the zero point.

The absence of local minima on the potential energy surface indicates that the concerted pathway is the energetically most favorable in the gas phase (see Fig. 3), which, in particular, casts doubt on the possibility of the formation of zwitterionic intermediate **8** in polar solvents in the route to products **4** as a result of the migration of the substituent.

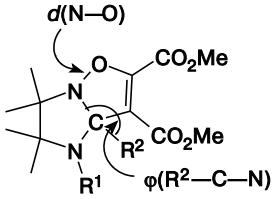

Fig. 4. Reaction coordinates: the *d*(N—O) bond length and the φ(R^2—C—N) bond angle.

The structures of the transition states of the rearrangements of **1c—j** into **4c—j**, respectively, were determined with the use of standard calculation methods (Fig. 5).

The geometric characteristics of the transition states, the calculated activation barriers ($\Delta G^{\#}_{298}$),* and the calculated free energies of the reactions ($\Delta G_r^{\circ}{}_{298}$) are given in Table 5.

The $\Delta G_r^{\circ}{}_{298}$ values indicate that this reaction is thermodynamically favorable and, consequently, irreversible. According to the Hammond postulate, exothermic reactions proceed through early transition states, which is in complete agreement with the above-described model. A comparison of the calculated and experimental $\Delta G^{\#}_{298}$ values shows that these values are in good quantitative agreement in the series of N-unsubstituted (**1d—f**) and N-methyl-substituted (**1g—i**) derivatives (Fig. 6). However, the difference in the calculated and experimental $\Delta G^{\#}_{298}$ values is 10 kcal mol^{-1}, which can be attributed to the fact that the experimentally observed solvent effect

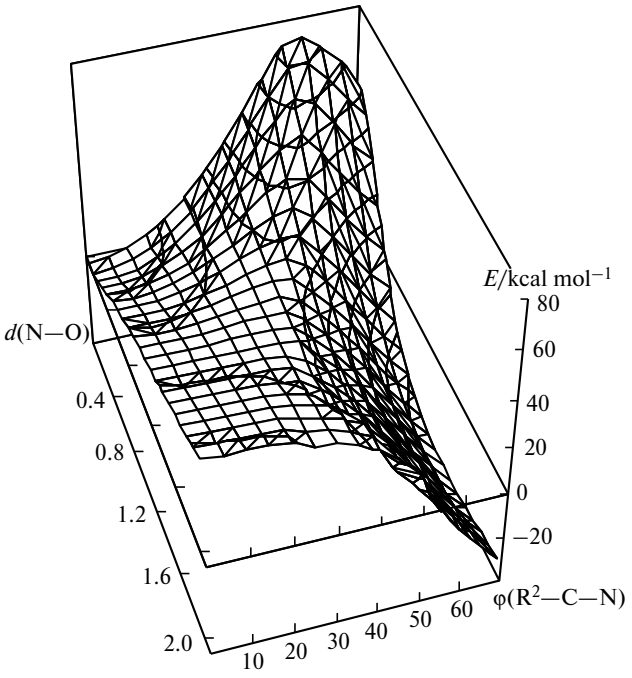

Fig. 3. Energy surface of the rearrangement of **1d** into **4d** in the bond length *d* (N—O)—bond angle φ(R^2—C—N) coordinates.

* $E_A = \Delta G^{\#}_{298}$ on the assumption of the isobaric-isothermal process.

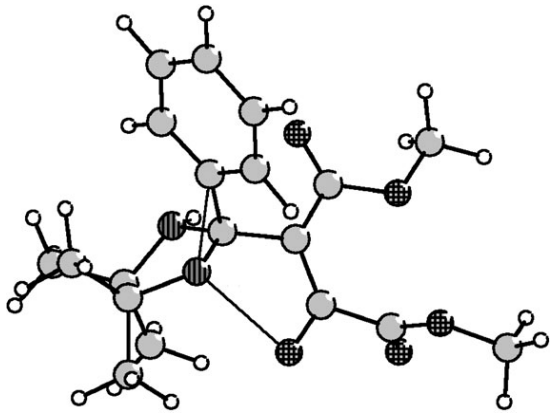

Fig. 5. Structure of the transition state of the rearrangement of compound **1d** into compound **4d**.

Table 5. Calculated activation barriers ($\Delta G^{\#}_{298}$), free energies of the reactions ($\Delta G_r^{\circ}{}_{298}$), and geometric characteristics (Δd, $\Delta\varphi$) of the transitions states of the rearrangements for compounds **1c—j**

Compound	$\Delta G^{\#}_{298}$	$\Delta G_r^{\circ}{}_{298}$	Δd(N—O) (Å)	$\Delta\varphi$(Ar—C—N)
	/kcal mol^{-1}			
1c	24.60	−47.76	0.953	32.443
1d	22.58	−48.20	0.960	32.052
1e	20.26	−48.09	0.964	31.514
1f	16.90	−48.57	0.966	30.14
1j	17.74	−50.38	—	—
1g	21.58	−48.55	0.932	30.051
1h	19.61	−47.87	0.930	29.617
1i	17.34	−51.06	0.926	28.898

Note. $\Delta G^{\#}_{298} = E_f^{\#} - E_f^{r}$, where E_f is the energy of the formation, $\Delta G_r^{\circ}{}_{298} = \Delta G_f^{\circ}{}_{298}^{p} - \Delta G_f^{\circ}{}_{298}^{r}$; $\Delta d = d^{\#} - d^{r}$; $\Delta\varphi = \varphi^{r} - \varphi^{\#}$; the superscripts r, p, and # refer to the reagents, the products, and the transition state, respectively.

was not taken into account in the calculations. The calculated sensitivities of the reaction ρ (calculated by the formula $\rho = [(\Delta G^{\#}_{298})_Z - (\Delta G^{\#}_{298})_H]/[2.303\sigma^{+}]$) are −1.4 ($R^1$ = H) and −1.3 (R^1 = Me) in the two reaction series under consideration, whereas the experimental ρ values are −3.2 and −2.3, respectively, *i.e.*, the calculations predicted the earlier transition state with the smaller charge separation and, consequently, with the lower sensitivity compared to the experimental value.

The overall situation is indicative of the correctness of the quantum mechanical model, which can be used for the quantitative estimation of experimental data in particular reaction series.

According to the results of calculations, the structure of the transition state is characterized by the longer breaking C(7a)—C(i) bond (1.669 Å) and the newly formed C(i)—N(4) bond (1.940 Å) (see Fig. 5). The typical bond lengths for the sp^3-hybridized centers[19] are 1.537 Å and 1.472 Å, respectively. Therefore, the transition states of the reactions *b* can be considered as σ complex **8** in the early step of its formation.

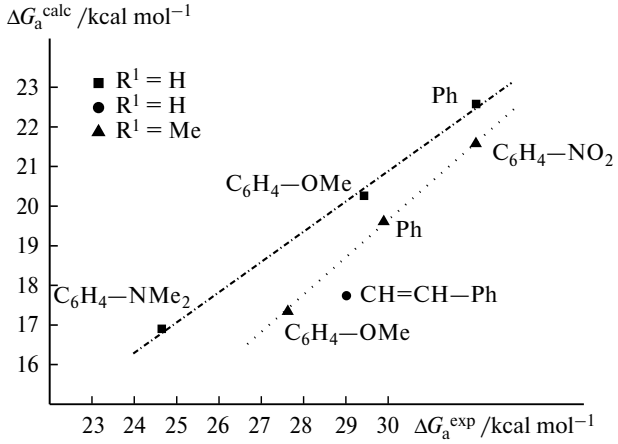

Fig. 6. Comparison of the experimental and calculated activation free energies ΔG_a for the reaction *b* (see Scheme 1) of compounds **1c—j**.

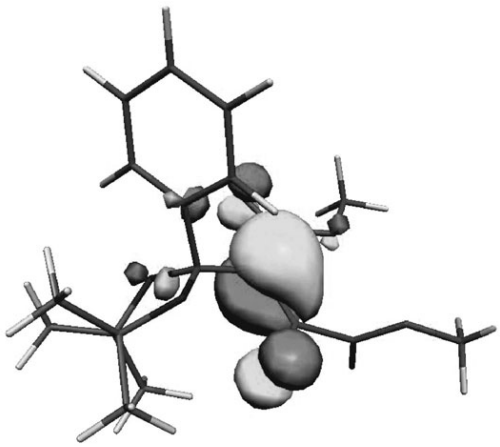

Fig. 7. Highest occupied molecular orbital of the transition state of the rearrangement of **1d** into **4d**.

The calculated activation barriers for N-methyl-substituted derivatives **1g—i** are, on the average, 3 kcal mol^{-1} lower than those of the corresponding N-unsubstituted compounds **1c—e** (see Table 5). This result is in agreement with the observed effect of this substituent (see Table 4). The observed increase in the rate of migration upon the introduction of the methyl group can be explained by considering the frontier orbitals of the transition state. The DFT calculations showed that the lone pair of the nitrogen atom N(1) makes a considerable contribution to HOMO of the transition state (Fig. 7), thus stabilizing the structure. The introduction of the methyl group R^1 increases the electron-releasing ability of the nitrogen atom N(1), resulting in the observed increase in the reaction rate.

In summary, we evaluated the influence of the polarity of the solvent and the structural factors on the rate of the rearrangement into 1,2,3,7a-tetrahydroimidazo[1,2-*b*]-isoxazole derivatives **1**. Based on the experimental data and the results of DFT calculations for the rearrangement associated with the migration of the substituent and the formation of dimethyl 2-oxo-3-(4,4,5,5-tetramethyl-1-arylimidazolidin-2-ylidene)succinate derivatives, the mechanism of the concerted process through the polar transition state was proposed.

Experimental

The ^{1}H NMR spectra were recorded on Bruker AM-400 and Bruker AV-300 spectrometers with the use of the signal of the

solvent as the internal standard. The ^{13}C NMR spectra were measured with complete decoupling from the constants J_{CH}. The IR spectra were recorded on a Bruker Vector-22 spectrometer in KBr pellets. The melting points were measured on a Boetius hot-stage apparatus. The elemental analysis of the compounds was carried out in the Laboratory of Microanalysis of the N. N. Vorozhtsov Novosibirsk Institute of Organic Chemistry of the Siberian Branch of the Russian Academy of Sciences. The course of the reactions was monitored by TLC on Silufol UV-254 plates and aluminum oxide/TLC cards (Fluka) with the use of chloroform, a chloroform—methanol mixture, and a hexane—ethyl acetate mixture as the eluents. The compounds were isolated by column chromatography on silica gel (Merck, Silica gel 60) or aluminum oxide (analytical grade, neutral, for chromatography). Chloroform of technical purity was dried over $CaCl_2$ and distilled. Hexane, ethyl acetate, and diethyl ether (high-purity grade) were used without additional purification. In all cases, the solutions were concentrated in a water-jet pump vacuum.

Quantum chemical calculations of the energies of the formation, the geometry, and the dipole moments for reagents **1c—j** and the transition states of their rearrangements into **4c—j** were carried out by the DFT method at the PBE level of theory[21] with the 3z basis set using the Priroda program.[22]

Compounds **1a—j** have been synthesized previously.[23,24] Compounds **1k—m** were synthesized in a similar way by the 1,3-dipolar cycloaddition of the nitrone 2-[(4-dimethylaminophenyl)]-4,4,5,5-tetramethyl-4,5-dihydro-1*H*-imidazole 1-oxide with alkynes. The syntheses of 2-[(4-dimethylaminophenyl)]-4,4,5,5-tetramethyl-4,5-dihydro-1*H*-imidazole 1-oxide[24] and compounds **3a—e**,**g**, **4g—i**, and **5d—f**,**j** have been described previously.[1] Alkynes, *viz.*, methyl 3-phenylprop-2-ynoate **11k**,[25] 4-phenylbut-3-yn-2-one **11l**,[26] and 3-phenylprop-2-ynenitrile **11m**,[27] were synthesized according to procedures described in the literature.

Methyl 7a-(4-dimethylaminophenyl)-2,2,3,3-tetramethyl-6-phenyl-1,2,3,7a-tetrahydroimidazo[1,2-*b*]isoxazole-7-carboxylate (1k). A solution of 2-[(4-dimethylaminophenyl)]-4,4,5,5-tetramethyl-4,5-dihydro-1*H*-imidazole 1-oxide (0.071 g, 0.27 mmol) and methyl 3-phenylprop-2-ynoate (0.050 g, 0.33 mmol) in $CHCl_3$ (1 mL) was refluxed for 6 h. The solvent was evaporated, and the residue was purified by chromatography on alumina with the use of chloroform as the eluent. The product was recrystallized from a hexane—ethyl acetate mixture. The yield was 0.082 g (74%), m.p. 124—125 °C (heptane). Found (%): C, 71.23; H, 7.33; N, 9.94. $C_{25}H_{31}N_3O_3$. Calculated (%): C, 71.23; H, 7.41; N, 9.97. ^1H NMR ($CDCl_3$), δ: 0.98, 1.12, 1.24, and 1.34 (all s, 3 H, C(2)Me, C(3)Me); 2.92 (s, 6 H, NMe_2); 3.48 (s, 3 H, CO_2Me); 6.66 (d, 2 H, CH arom., ^3J = 9.0 Hz); 7.35—7.43 (m, 3 H, CH arom.); 7.56 (d, 2 H, CH arom., ^3J = 9.0 Hz); 7.62—7.65 (m, 2 H, CH arom.). IR (KBr), ν/cm^{-1}: 3345, 3063, 2980, 2945, 2805, 1702, 1643, 1611, 1522, 1437, 1340, 1165, 1117, 1070.

1-[7a-(4-Dimethylaminophenyl)-2,2,3,3-tetramethyl-6-phenyl-1,2,3,7a-tetrahydroimidazo[1,2-*b*]isoxazol-7-yl]ethanone (1l). A solution of 2-[(4-dimethylaminophenyl)]-4,4,5,5-tetramethyl-4,5-dihydro-1*H*-imidazole 1-oxide (0.110 g, 0.42 mmol) and 4-phenylbut-3-yn-2-one (0.073 g, 0.51 mmol) in toluene (1 mL) was stirred at room temperature for 12 h. The solvent was evaporated, and the residue was chromatographed on alumina with the use of chloroform as the eluent. The product was recrystallized from hexane. The yield was 0.11 g (65%), m.p. 127—128 °C (heptane). Found (%): C, 74.09; H, 8.03; N, 10.44. $C_{25}H_{31}N_3O_2$. Calculated (%): C, 74.04; H, 7.70; N, 10.36. ^1H NMR ($CDCl_3$), δ: 0.99, 1.13, 1.24, and 1.32 (all s, 3 H, C(2)Me, C(3)Me); 1.78 (s, 3 H, COMe); 2.91 (s, 6 H, NMe_2); 6.66 (d, 2 H, CH arom., ^3J = 8.9 Hz); 7.40—7.47 (m, 3 H, CH arom.); 7.51—7.54 (m, 2 H, CH arom.); 7.56 (d, 2 H, CH arom., ^3J = 8.9 Hz). ^{13}C NMR ($CDCl_3$), δ: 18.6, 24.4, 25.2, 25.8, 29.4, 40.1, 63.1, 71.6, 93.2, 111.2, 119.7, 126.8, 128.2, 128.6, 130.3, 133.1, 149.1, 161.2, 193.8. IR (KBr), ν/cm^{-1}: 3357, 2975, 2804, 1676, 1610, 1522, 1491, 1445, 1366, 1333, 1229, 1160, 1101, 1064, 1032.

7a-(4-Dimethylaminophenyl)-2,2,3,3-tetramethyl-6-phenyl-1,2,3,7a-tetrahydroimidazo[1,2-*b*]isoxazole-7-carbonitrile (1m). A solution of 2-[(4-dimethylaminophenyl)]-4,4,5,5-tetramethyl-4,5-dihydro-1*H*-imidazole 1-oxide (0.085 g, 0.33 mmol) and 3-phenylprop-2-ynenitrile (0.034 g, 0.27 mmol) in a mixture of toluene (2.5 mL) and $CHCl_3$ (2.5 mL) was heated at 65 °C for 3 h. The solvent was evaporated, and the product was purified by chromatography on alumina with the use of a hexane—ethyl acetate mixture (4 : 1) as the eluent. The reaction product crystallized after the addition of hexane, and the precipitate was filtered off. The yield was 0.028 g (28%), m.p. 148—150 °C (heptane). Found (%): C, 74.73; H, 7.47; N, 14.40. $C_{24}H_{28}N_4O$. Calculated (%): C, 74.20; H, 7.26; N, 14.42. ^1H NMR ($CDCl_3$), δ: 1.01, 1.11, 1.18, and 1.46 (all s, 3 H, C(2)Me, C(3)Me); 2.94 (s, 6 H, NMe_2); 6.72 (d, 2 H, CH arom., ^3J = 9.09 Hz); 7.38—7.45 (m, 3 H, CH arom.); 7.56 (d, 2 H, CH arom., ^3J = 9.0 Hz); 7.83—7.86 (m, 2 H, CH arom.). ^{13}C NMR ($CDCl_3$), δ: 18.9, 24.6, 24.9, 25.4, 40.1, 63.9, 72.5, 94.0, 111.9, 115.9, 125.5, 125.9, 126.5, 128.4, 130.9, 131.2, 149.8, 160.5. IR (KBr), ν/cm^{-1}: 3324, 3005, 2975, 2931, 2809, 2207, 1646, 1611, 1525, 1494, 1447, 1369, 1332, 1232, 1196, 1161.

Thermolysis of tetrahydroimidazoisoxazoles 1k—m (general procedure). A solution of compound **1** (0.1—0.2 mmol) in toluene (1—3 mL) was heated in a sealed tube. Then the solvent was concentrated. Products **4** and **5** were purified by chromatography and/or recrystallization.

Methyl 2-[1-(4-dimethylaminophenyl)-4,4,5,5-tetramethylimidazolidin-2-ylidene]-3-oxo-3-phenylpropanoate (4k) was synthesized from **1k** (0.020 g) at 150 °C during 6 h and purified by recrystallization from hexane; the yield was 0.010 g (50%), m.p. 156—158 °C (hexane). Found (%): C, 71.23; H, 7.33; N, 9.94. $C_{25}H_{31}N_3O_3$. Calculated (%): C, 70.91; H, 7.37; N, 10.23. ^1H NMR ($CDCl_3$), δ: 1.10 and 1.31 (both s, 6 H, C(4)Me, C(5)Me); 2.86 (s, 6 H, NMe_2); 2.98 (s, 3 H, CO_2Me); 6.47 (d, 2 H, CH arom., ^3J = 8.9 Hz); 6.78 (d, 2 H, CH arom., ^3J = 8.9 Hz); 7.18—7.21 (m, 3 H, CH arom.); 7.32—7.34 (m, 2 H, CH arom.); 9.80 (br.s, 1 H, NH). IR (KBr), ν/cm^{-1}: 3196, 3046, 2973, 2942, 2806, 1711, 1611, 1569, 1510, 1477, 1445, 1391, 1361, 1266, 1230, 1191, 1158, 1087.

X-ray diffraction study. Single crystals of compound **4k** suitable for the X-ray diffraction study were obtained by recrystallization from hexane. The measurements were carried out on an Oxford Diffraction KM4 single-crystal diffractometer equipped with a CCD detector (Mo-Kα radiation, λ = 0.71073 Å, graphite monochromator, ω-scanning technique) at room temperature. The empirical multiscan absorption correction was applied based on equivalent reflections (T_{min} = 0.902, T_{max} = 0.996). The X-ray diffraction data were collected and processed with the use of the *CrysAlisPro* program package.[28] Crystallographic data and the structure refinement statistics for compound **4k** are given in

Table 6. The structure was solved by direct methods and refined by the full-matrix least-squares method with the use of the *SHELX-97* program package[29] and the *WinGX* software package.[30] All nonhydrogen atoms were refined with anisotropic displacement parameters. The hydrogen atoms were positioned geometrically and refined using a riding model. The C—C distances were not sufficiently accurately refined because of the relatively high temperature factors of the carbon atoms of one of the phenyl rings (C(7)—C(8)—C(9)—C(10)—C(11)—C(12)), the geometry of this ring was fixed (the distances were 1.39 Å; the angles were 120°), and only the thermal parameters of the carbon atoms were refined. The structure was deposited with the Cambridge Crystallographic Data Centre (CCDC 748018) and can be obtained, free of charge, on application to www.ccdc.cam.ac.uk/data_request/cif.

2-[1-(4-Dimethylaminophenyl)-4,4,5,5-tetramethylimidazolidin-2-ylidene]-1-phenylbutane-1,3-dione (4l) and 2-[4,4,5,5-tetramethyl-2-(4-dimethylaminophenyl)-1-phenyl-4,5-dihydro-1*H*-3-λ-5-imidazol-3-ylidene]ethanone (3l′) were synthesized from **1l** (0.031 g) at 131 °C during 6.5 h and purified by chromatography on silica gel with the use of a $CHCl_3$—MeOH mixture (100 : 1) as the eluent followed by recrystallization from hexane. The yields of **4l** (m.p. 161—163 °C) and **3l′** (m.p. 213—215 °C) were 0.015 g (50%) and 0.007 g (25%), respectively.

Compound **4l**. Found *m/z* 405.2413 $[M]^+$. $C_{25}H_{31}N_3O_2$. Calculated M = 405.2411. ^{1}H NMR ($CDCl_3$), δ: 0.97 and 1.27 (both s, 6 H, C(4)Me, C(5)Me); 2.15 (s, 3 H, COMe); 2.86 (s, 6 H, NMe_2); 6.21 (d, 2 H, CH arom., ^3J = 9.0 Hz); 6.27 (d, 2 H, CH arom., ^3J = 9.0 Hz); 7.14—7.17 (m, 2 H, CH arom.); 7.22—7.25 (m, 2 H, CH arom.); 7.30—7.34 (m, 1 H, CH arom.); 10.73 (br.s, 1 H, NH). ^{13}C NMR ($CDCl_3$, 50.32 MHz), δ: 21.1, 23.2, 28.2, 40.1, 62.5, 67.5, 95.9, 111.7, 125.6, 127.1, 128.3, 128.6, 130.9, 140.9, 148.6, 163.2, 193.3, 194.3.

Table 6. Crystallographic parameters and the X-ray diffraction data collection and structure refinement statistics

Molecular formula	$C_{25}H_{31}N_3O_3$
Molecular weight	421.53
Crystal system	Triclinic
Space group	*P*1
a/Å	10.7797(11)
b/Å	11.0239(11)
c/Å	12.3057(12)
α/deg	114.583(10)
β/deg	101.122(9)
γ/deg	107.597(9)
V/Å^3	1178.8(2)
Z	2
d_{calc}/g cm^{-3}	1.188
μ/cm^{-1}	0.079
θ-Scan range/deg	3.16—25.35
Number of measured reflections	8141
Number of independent reflections	4194 (R_{int} = 0.0611)
Number of reflections with $I > 2\sigma(I)$	1229
Number of refined parameters	275
$R_1(F^2 > 2\sigma(F^2))$	0.0564
$wR_2(F^2)$ based on all reflections	0.1622

Compound **3l′**. Found *m/z* 363.2301 $[M]^+$. $C_{23}H_{29}N_3O$. Calculated M = 363.2305. ^{1}H NMR ($CDCl_3$), δ: 1.11 and 1.32 (both s, 6 H, C(4)Me, C(5)Me); 3.00 (s, 6 H, NMe_2); 4.91 (s, 1 H, H(2)); 6.7 (d, 2 H, CH arom., ^3J = 8.9 Hz)); 7.04 (d, 2 H, CH arom., ^3J = 8.9 Hz); 7.25—7.28 (m, 3 H, CH arom.); 7.66—7.69 (m, 2 H, CH arom.); 9.63 (br.s, 1 H, NH). ^{13}C NMR ($CDCl_3$, 50.32 MHz), δ: 21.1, 23.7 40.5, 62.2, 67.5, 74.9, 112.3, 124.3, 126.7, 127.8, 129.5, 131.1, 141.6, 150.0, 162.9, 185.1. IR (KBr), ν/cm^{-1}: 2977, 2887, 2805, 1607, 1593, 1572, 1524, 1446, 1404, 1367, 1291, 1211, 1186, 1155, 1134.

2-[1-(4-Dimethylaminophenyl)-4,4,5,5-tetramethylimidazolidin-2-ylidene]-3-oxo-3-phenylpropanenitrile (4m) and 2-[2-(4-dimethylaminophenyl)-4,4,5,5-tetramethyl-4,5-dihydro-1*H*-3-λ-5-imidazol-3-ylidene]-3-oxo-3-phenylpropanenitrile (3m) were synthesized according to the general procedure from **1m** (0.031 g) at 131 °C during 7.5 h. The product was purified by column chromatography on silica gel. Compound **4m**, $CHCl_3$—MeOH (80 : 1) as the eluent, the yield was 0.017 g (55%), m.p. 280—282 °C. Compound **3m**, $CHCl_3$—MeOH (10 : 1) as the eluent, the yield was 0.007 g (23%), m.p. 298—300 °C.

Compound **4m**. Found *m/z* 388.2251 $[M]^+$. $C_{24}H_{28}N_4O$. Calculated M = 388.2258. ^{1}H NMR ($CDCl_3$), δ: 1.15 and 1.35 (both s, 6 H, C(4)Me, C(5)Me); 2.96 (s, 6 H, NMe_2); 6.67 (d, 2 H, CH arom., ^3J = 9.0 Hz); 7.04 (d, 2 H, CH arom., ^3J = 9.0 Hz); 7.25—7.31 (m, 3 H, CH arom.); 7.60—7.62 (m, 2 H, CH arom.); 10.23 (br.s, 1 H, NH). ^{13}C NMR ($CDCl_3$, 50.32 MHz), δ: 20.8, 23.3, 39.9, 62.4, 68.5, 66.9, 111.4, 119.3, 122.4, 125.6, 127.2, 127.5, 130.8, 129.7, 139.9, 150.4, 162.4, 192.2. IR (KBr), ν/cm^{-1}: 3225, 2985, 2918, 2817, 2191, 1611, 1589, 1539, 1524, 1479, 1447, 1368, 1345, 1290, 1175, 1153, 1128, 702.

Compound **3m**. Found *m/z* 388.2254 $[M]^+$. $C_{24}H_{28}N_4O$. Calculated M = 388.2258. ^{1}H NMR ($CDCl_3$), δ: 0.77 and 1.20 (both s, 3 H, C(4)Me, C(5)Me); 1.26 (s, 6 H, C(4)Me, C(5)Me); 2.94 (s, 6 H, NMe_2); 6.44 (d, 2 H, CH arom., ^3J = 9.1 Hz); 7.14—7.18 (m, 3 H, CH arom.); 7.35—7.37 (m, 2 H, CH arom.); 7.78 (d, 2 H, CH arom., ^3J = 9.0 Hz); 10.93 (br.s, 1 H, NH). IR (KBr), ν/cm^{-1}: 2976, 2923, 2732, 2161, 1611, 1576, 1539, 1512 1437, 1385, 1299, 1205, 1174, 1141.

Determination of the reaction rate constant (general procedure). A solution of compound **1** (5—50 mg) in a solvent (0.5 mL) was placed in a sealed glass tube (in the case of a deuterated solvent, in a carefully sealed NMR tube) and kept at 20—150 °C. The reaction time was varied from 1 to 80 h. Then the tube was broken, the solvent was evaporated (except the cases of the deuterated solvents), and the ^{1}H NMR spectra of the mixtures were recorded. The rate constants k_a and k_b were evaluated by the equations (1) and (2). These operations were repeated 2—4 times at one temperature and at different reaction times.

References

1. N. V. Chukanov, S. A. Popov, G. V. Romanenko, V. A. Reznikov, *Tetrahedron*, 2008, **64**, 7432.
2. J. P. Freeman, *Chem. Rev.*, 1983, **83**, 241.
3. H. Seidl, R. Huisgen, *Chem. Ber.*, 1969, **102**, 904.
4. R. M. Acheron, A. S. Bailey, I. A. Selby, *J. Chem. Soc. (C)*, 1967, **20**, 2066.
5. S.Takahashi, H. Kano, *J. Org. Chem.*, 1965, **30**, 1118.
6. F. Heaney, T. McCarthy, M. Mahon, V. McKee, *Org. Biomol. Chem.*, 2005, **3**, 4351.

7. N. Coskun, S. Tuncman, *Tetrahedron*, 2006, **62**, 1345.
8. T. A. Berezina, V. A. Reznikov, L. B. Volodarskii, I. Ya. Bagryanskaya, Yu. V. Gatilov, *Izv. Akad. Nauk, Ser. Khim.*, 2000, 112 [*Russ. Chem. Bull., Int. Ed.*, 2000, **49**, 116].
9. A. Padwa, M. Meske, Z. Ni, *Tetrahedron*, 1995, **51**, 89.
10. B. Alcaide, E. Saez, *Tetrahedron Lett.*, 2000, **41**, 1647.
11. R. C. F. Jones, J. N. Martin, P. Smith, T. Gelbrich, M. E. Light, M. B. Hursthouse, *Chem. Commun.*, 2000, **19**, 1949.
12. M. L. M. Pennings, G. Okay, D. N. Reinhoudt, S. Harkema, G. J. Van Hummel, *J. Org. Chem.*, 1982, **47**, 4413.
13. R. Huisgen, H. Giera, K. Polborn, *Liebigs Ann./Recueil*, 1997, **8**, 1691.
14. Y. Kobayashi, I. Kumadaki, T. Yoshida, *Heterocycles*, 1977, **8**, 387.
15. J. P. Freeman, D. J. Duchamp, C. G. Chidester, G. Slomp, J. Szmuszkovicz, M. Raban, *J. Am. Chem. Soc.*, 1982, **104**, 1380.
16. R. Gree, R. Carrie, *J. Am. Chem. Soc.*, 1977, **99**, 6667.
17. R. Huisgen, K. Niklas, *Heterocycles*, 1984, **22**, 21.
18. *The Chemist´s Companion: A Handbook of Practical Data, Techniques and References*, Ed. A. J. Gordon, R. A. Ford, Wiley, New York, 1972, 311 pp.
19. A. S. Dneprovskii, T. I. Temnikova, *Teoreticheskie osnovy organicheskoi khimii* [*Theoretical Fundamentals of Organic Chemistry*], Khimiya, Leningrad, 1979, 520 pp. (in Russian).
20. H.Takeuchi, T. Taniguchi, T. Ueda, *J. Chem. Soc., Perkin. Trans. 2*, 2000, **2**, 295.
21. J. P. Perdew, K. Burke, M. Ernzerhof, *Phys. Rev. Lett.*, 1996, **77**, 3865.
22. D. N. Laikov, *Chem. Phys. Lett.*, 1997, **281**, 151.
23. S. A. Popov, N. V. Chukanov, G. V. Romanenko, T. V. Rybalova, Y. V. Gatilov, V. A. Reznikov, *J. Heterocycl. Chem.*, 2006, **43**, 277.
24. N. V. Chukanov, S. A. Popov, G. V. Romanenko, V. A. Reznikov, *Izv. Akad. Nauk, Ser. Khim.*, 2007, 1182 [*Russ. Chem. Bull., Int. Ed.*, 2007, **56**, 1227].
25. V. L. Heasley, D. F. Shellhamer, A. E. Chappell, J. M. Cox, D. J. Hill, S. L. McGovern, C. C. Eden, *J. Org. Chem.*, 1998, **63**, 4433.
26. P. Simunek, V. Bertolasi, M. Peskova, V. Machacek, A. Lycka, *Org. Biomol. Chem.*, 2005, **3**, 1217.
27. H. Adkins, G. M. Whitman, *J. Am. Chem. Soc.*, 1942, **64**, 150.
28. Oxford Diffraction, *CrysAlisPro*, Oxford Diffraction Ltd., Abingdon, England, 2008.
29. G. M. Sheldrick, *Acta Crystallogr. Sec. A*, 2008, **64**, 112.
30. L. J. Farrugia, *J. Appl. Crystallogr.*, 1999, **32**, 837.

Received October 15, 2009;
in revised form July 8, 2010